Sensors and Materials, Vol. 13, No. 7 (2001) 385–397
MYU Tokyo

S & M 0458

Properties of Magnetorheologic Fluids

L. Richter, L. Zipser* and U. Lange

HTW, University of Applied Sciences Dresden,
Friedrich-List-Platz 1, D–01069 Dresden, Germany

(Received December 18, 2000; accepted July 6, 2001)

Key words: magnetorheologic fluids, permeability, viscosity

A feasible model for efficiently describing the flow of magnetorheological fluids (MRF) in narrow channels, based on the Bingham equation, is presented. This model permits an accurate determination of shear stress τ, yield point τ_f and Bingham viscosity η_B at high shear rates $\dot{\gamma}$ so far not investigated. These parameters are calculated from pressure difference Δp and volume flow $\dot{V}$, measured under variable process conditions. Furthermore, the frequency characteristic of the relative permeability μ_r of MRFs is investigated in the industrially significant range up to 1500 Hz.

1. Introduction

Magnetorheologic fluids are suspensions of soft-magnetic particles about 1 to 5 μm in diameter suspended in special oils.[1,2] The particles are covered with a thin non-magnetic film which prevents agglomeration. The weight percentage of the particles in the suspension is about 80% at a total density of 3 g/cm^3. A raster-electron microscope (REM) view of the particles is shown in Fig. 1. Without a magnetic field the particles are statistically distributed. Under the influence of a magnetic field the particles line up in chains; this behaviour is the "magnetorheologic effect." If an external force or pressure is applied, the chains are deformed as shown in Fig. 2.[3] In the shear mode a) the chains resist the displacement of the bordering plates. In the flow mode b) the chains are deformed and resist the applied pressure. In the squeeze mode c) the chains prevent the draining away of the fluid. Most interesting for applications in actuators is the flow mode. In this case under the influence of a magnetic field the magnetorheologic fluid changes its flow behaviour

*Corresponding author, e-mail: zipser@et.htw-dresden.de

Fig. 1. REM view of the ferromagnetic particles of magnetorheologic fluids.

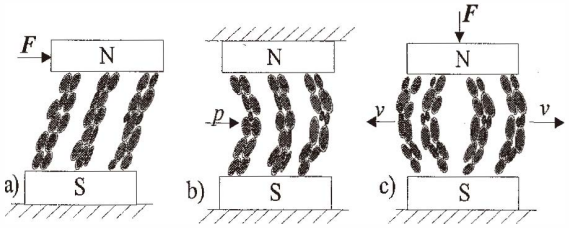

Fig. 2. Stress modes of magnetorheologic fluids.

from Newtonian to Bingham characteristics. The Bingham flow is described as in ref. 4

$$\tau(B,\dot{\gamma},\eta) = \tau_f(B) + \eta_B \cdot \dot{\gamma}, \tag{1}$$

with shearing stress τ, magnetic flux density B, Bingham viscosity η_B and shearing rate $\dot{\gamma}$. A graphic presentation of (1) is given in Fig. 3. Without a magnetic field, when $B = 0$, the MRF is a conventional Newtonian fluid. For $B > 0$ the MRF is a Bingham fluid, with the result that a shearing stress τ emerges. For values $\tau < \tau_f$ the MRF behaves like a solid (area 1 in Fig. 4). Only at higher shearing stress $\tau > \tau_f$ does the MRF behave like a fluid (area 2 in Fig. 4).[5] This interesting viscoelastic behaviour can be used in actuators for the controlled damping of moving parts or for the control of fluid flow in narrow channels.

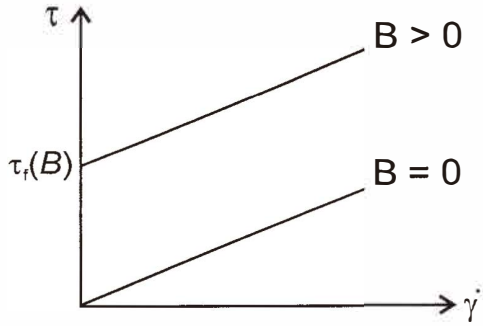

Fig. 3. Graphic presentation of the Bingham eq. (1).

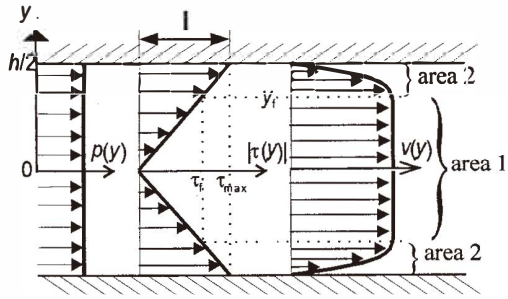

Fig. 4. Distributions of pressure $p(y)$, shearing stress $\tau(y)$ and flow velocity $v(y)$ across a channel.

2. Set-up for Experimental Investigation of MRFs

For the precise determination of the static rheologic parameters τ, η and $\dot{\gamma}$ of MRFs an experimental apparatus was constructed (Fig. 5).[6] The MRF is pressed through a narrow rectangular channel 10 mm wide and with a variable height of 0.5, 1 or 2 mm. In the measuring process, pressure difference $\Delta p = p_1 - p_2$, magnetic flux density B and temperature T are determined. During one measurement cycle, the streaming MRF in the measuring channel is exposed to a magnetic field of constant flux density B in a defined active region A_B of 10×10 mm^2.

In this way, the fluid resistance and, in consequence, the pressure difference $\Delta p = p_1 - p_2$ across the region A_B rises significantly as a result of the magnetorheological effect. Before starting a measurement, the MRF element, the hydraulic pipes and cylinders are tempered to an equal temperature in a climatic chamber. Moreover, to avoid possible sedimentation, the MRF is repeatedly pressed through the measuring element. Figure 6 shows one measuring cycle for piston shift $s(t)$ and measured pressures $p_2(t)$ and $p_1(t)$.

The time variations of $s(t)$, $p_1(t)$ and $p_2(t)$ are nearly constant within one measurement. Because of the unavoidable clearance of about 30 mm, the piston shift $s(t)$ is not uniform at

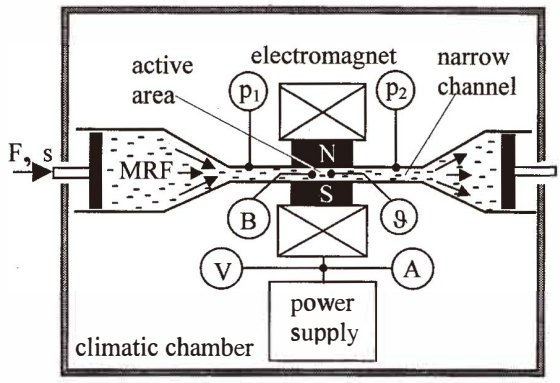

Fig. 5. Schematic of the experimental setup.

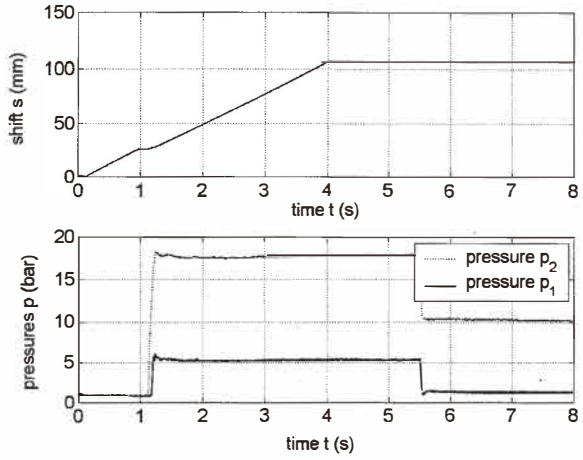

Fig. 6. Shift $s(t)$ and pressures $\Delta p_2(t)$ and $\Delta p_1(t)$ for one measuring cycle.

about $t = 1.3$ s. This appears as a short decrease in the slope of the distance vs time line. Only after this time t are the piston of the hydraulic cylinder and consequently the MRF in the narrow channel set into uniform motion. For the extraction of measured values with the aid of evaluating programs only the uniform part of the distance-time graph is used. For constructive reasons the measuring points for pressures p_1 and p_2 must be arranged at a certain distance from the active region A_B (see Fig. 5). The resultant total pressure error $\Delta(\Delta p)$ is corrected by a linear interpolation. Not until the measuring cycle of $t = 5.5$ s is finished is the magnetic field switched off. Therefore a pressure difference $\Delta p = 10$ bar remains for $t > 5.5$ s.

3. Results of the Measurements

As examples, two sets of results at the temperatures 20°C and 80°C are shown in Figs. 7 and 8. The dispersion of the measured values is probably due to local temperature effects resulting from the transformation of mechanical into thermal energy.[7]

Such temperature effects have to be considered in designing magnetorheologic actuators. For small flux densities, $B \leq 3$ mT, the MRF is considered to be demagnetised and

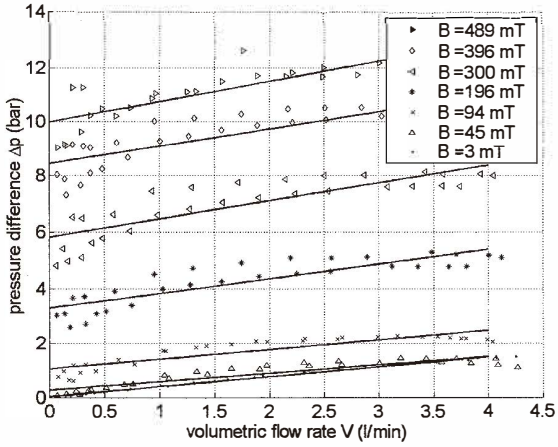

Fig. 7. Measured characteristics for the MRF 132LD (Lord Corp.) at temperature $\theta = 20$°C and channel height $h = 1$ mm.

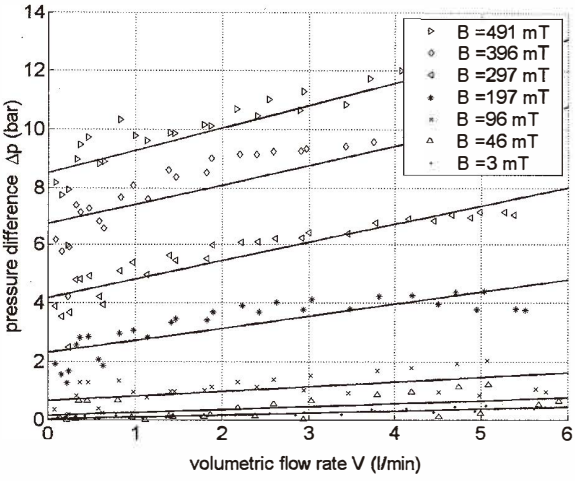

Fig. 8. Measured characteristics for the MRF 132LD (Lord Corp.) at temperature $\theta = 80$°C and channel height $h = 1$ mm.

behaves like a Newtonian fluid. Stronger magnetic fields with $B > 3$ mT cause a shift of the $\Delta p/\dot{V}$ –characteristic along the ordinate. For applications in actuators and dampers, the flow resistance R_{MRF} of an MRF-filled channel in a magnetic field is of interest. The measured characteristics in Figs. 7 and 8 represent the resistivity profile of such a resistor R_{MRF}. At very high flow velocities v of the MRF, the magnetorheologic effect could probably be reduced because there is not sufficient time for the formation of particle chains. In actual experiments, maximal velocities of $v \approx 7$ m/s were reached. This corresponds to a dwell time as short as 1.5 ms in the active region A_B. Despite this short time, the magnetorheologic effect is significant. Presumably, such short dwell times are sufficient in most actuators. Figures 7 and 8 confirm that the MRF under the influence of a magnetic field begins to flow only if a minimal pressure difference Δp_f is exceeded. This pressure difference is the yield point $\tau_f(B)$.

4. Characteristics of Magnetorheologic Fluids

According to ref. 8, under technically reasonable conditions, with the shearing stress

$$\dot{\gamma}(y) = \frac{dv(y)}{dy}, \tag{2}$$

from eq. (1) the v- profile in area 2 of Fig. 4 follows the following equation:

$$v(y) = -\frac{\Delta p}{2\eta_B l} y^2 - \frac{\tau_f}{\eta_B} y + \frac{h}{2\eta_B}(\tau_f + \frac{\Delta p h}{4l}). \tag{3}$$

The maximum shearing stress, before the MRF begins to flow, is the observed yield point

$$\tau_f(B) = -\frac{\Delta p_f(B)}{l}\frac{h}{2}. \tag{4}$$

From the measured pressure difference Δp, volume flow $\dot{V}$ and the geometric parameters l, b and h of the channel, the resulting Bingham viscosity,

$$\eta_B = \frac{bh^3}{24\dot{V}l}\left(2\Delta p - 3\Delta p_f + \frac{\Delta p_f{}^3}{\Delta p^2}\right), \tag{5}$$

can be calculated. Finally, the shearing rate,

$$\dot{\gamma}(y) = -\frac{1}{\eta_B}\left(\frac{\Delta p}{l} y - \frac{\Delta p_f}{l}\frac{h}{2}\right), \tag{6}$$

can be determined in an analogous way. Using eqs. (3) to (6), from the measured values the Bingham functions of the investigated MRF can be calculated. For the results of Figs. 7 and 8 the plots of the Bingham functions are shown in Fig. 9. For a flux density $B > 0$, a linear approximation of the Bingham function is permitted,

$$\tau(B,\dot{\gamma}) = \tau_f(B) + \eta_B \cdot \dot{\gamma} = a + b \cdot \dot{\gamma}, \tag{7}$$

with the regression coefficients a and b which depend on the flux density B.

5. Temperature Dependence of MRFs

A comparison of Figs. 7 and 8 shows that the properties of MRFs depend strongly on the temperature T. An MRF without a magnetic field behaves like an ordinary Newtonian fluid. Its temperature dependence can be described by the Vogel eq. (9) (see Fig. 10). The measured results, determined with the experimental setup described above, conform well with results that were determined with conventional rotational viscometers. In the Bingham eq. (7) viscosity η_B does not depend on magnetic flux density B. However, the measured results illustrate that a remarkable nonlinear dependence exists (Fig. 11). For investigating the temperature dependence of the yield point $\tau_f(B)$, the regression coefficients a in (7) are plotted as a function of the absolute temperature T together with flux density B (Fig. 12). The yield point $\tau_f(B)$ decreases proportionally with the absolute temperature T in the investigated interval of the flux density B. This correlation can be described by a modified Vogel equation,

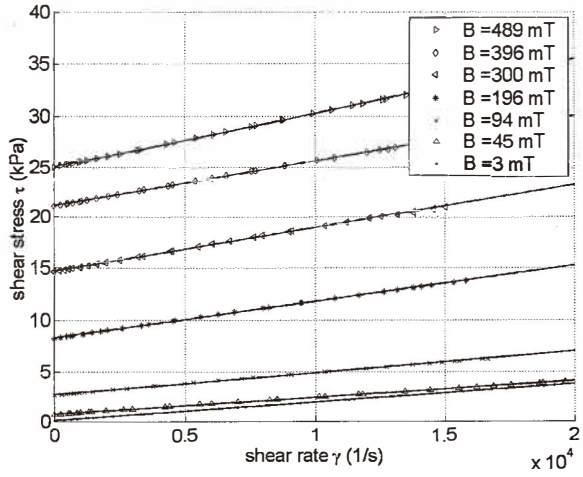

Fig. 9. Approximated Bingham functions of the MRF 132LD.

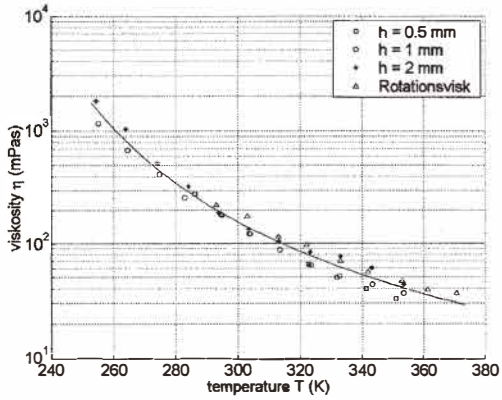

Fig. 10. Newtonian viscosity η_N of the MRF 132LD.

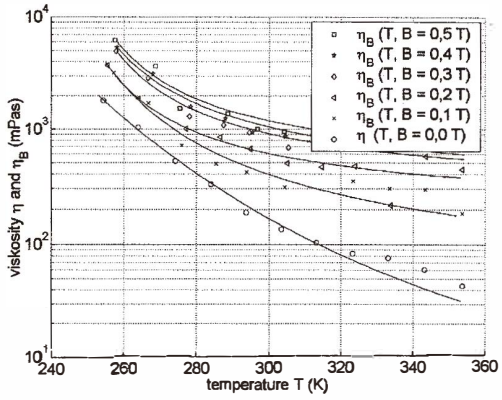

Fig. 11. Dependence of the viscosity of MRF 132 LD on temperature T.

$$\tau_f(T) = ae^{\frac{b}{T+c}}. \tag{8}$$

The coefficient a and the constants b and c can be determined by approximation only for constant magnetic flux density B. For designing magnetorheologic devices the strong temperature dependence of the viscosity η, particularly at low temperatures, has to be considered.

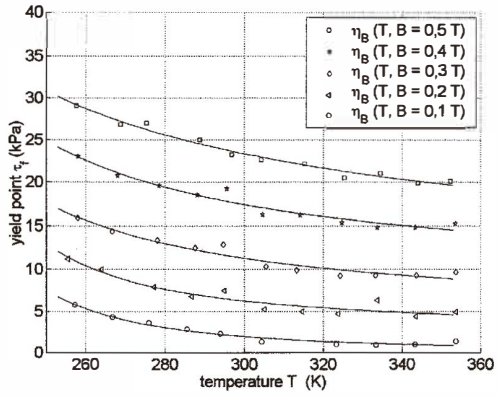

Fig. 12. Dependence of yield point $\tau_f(B)$ on absolute temperature T for MRF 132LD.

6. Relative Permeability of MRFs

The measuring setup for determining the dependence of the relative permeability μ_r on the frequency f consists of two solenoids nested within one another, a measuring coil and an exciting coil. The MRF probe is situated in the centre of the solenoids. The measuring coil is bifilarly wrapped. A power supply activates the exciting coil with different frequencies f. The effective values of the exciting current i_{exc} and the induced voltage u_{ind} are measured. For determining the exciting magnetic field H_{exc} and the induced flux density B_{ind}, the probe is assumed to be infinitely long. According to Ampere's law the magnetic field in the exciting coil is as in eqs. (10) and (11):

$$H_{exc} = \frac{K \cdot i_{exc}}{\mu_0}, \tag{9}$$

and

$$B_{ind} = \frac{50}{f}\frac{50}{A_{MRF}N}|u_{ind}| + \mu_0 H_{ind}. \tag{10}$$

The term A_{MRF} is the winding cross section of the measuring coil and N is the number of windings. The dependence of the magnetic flux density B_{ind} on the field H_{ind} is shown in Fig. 13.

In the frequency interval considered, $20 \leq f \leq 1500$ Hz, no frequency dependence of B_{ind} is perceptible. On the other hand a significant influence of the magnetic field H_{ind} exists on the relative permeability μ_r (Fig. 14). The maximum value of $\mu_r \approx 6$ is reached at a field intensity of about $H_{ind} = 10^4$ A/m. The value of μ_r attained is approximately the same for all investigated MRFs.

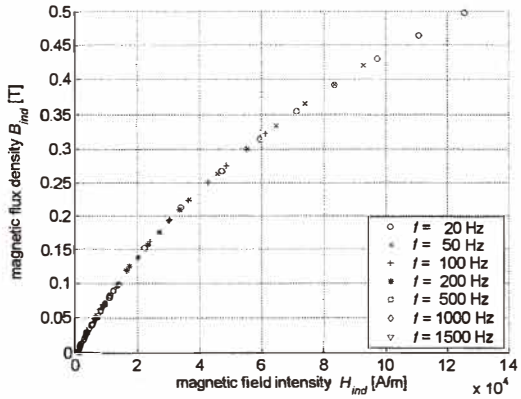

Fig. 13. Magnetic flux density B_{ind} as a function of field Hind.

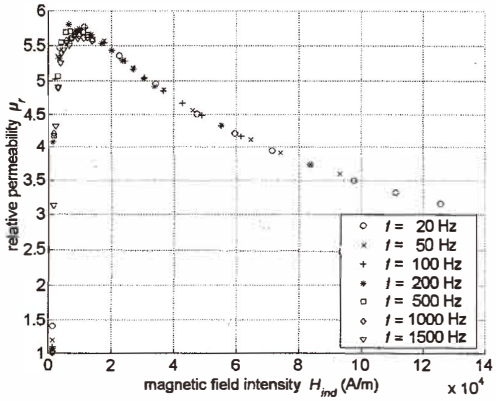

Fig. 14. Dependence of the relative permeability μ_r on field Hind of the MRF 132LD.

7. Existing and Potential Future Applications

The outstanding feature of MRFs is their directly electrically controllable flow. Resulting from this, new types of electromagnetically controllable dampers and breaks can be designed. First examples are a seismic damper,[12] a suspension seat for agricultural engines[13] and a smart adaptive prosthesis.[14] Vibration dampers for cars and washing machines are under development. Furthermore, in the future even adaptive end-impact dampers or dampers for the reduction of vibrations in microsystems or otherwise in large engine foundations could be realised.

A miniaturised end-impact damper for the improved soft switching of small magnetic valves with a maximum stroke $s = 400$ μm is shown in Fig. 15. The exact measurement and

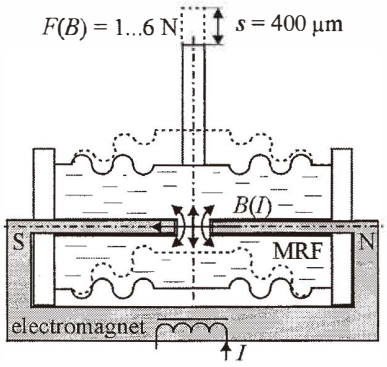

Fig. 15. Miniaturised end-impact damper.

control of this stroke is expensive. The damper has to realise a time-dependent damping force along an extremely small distance. The damping force F depends on the electrically generated magnetic flux density B and is changeable from 1 N to 6 N. The effective MRF volume in the damper is only 0.025 ml and is bordered by two membranes with a diameter of 10 mm. The diameter of the 'flow channel' is only 1 mm. Figure 16 shows the damping characteristics $s(t)$ of the miniaturised damper for different small supply currents $I = 0....50$ mA. The external force F is 3.2 N.

Obviously, with a small control energy it is already possible to influence significantly the damping characteristic of the damper. For small forces $F < 2$ N and currents $I > 20$ mA a hysteresis can be observed, i.e., the full elongation $s = 400$ µm will not be reached. This shows limits in the application of magnetorheologic fluids for miniaturised dampers.

8. Conclusions

For the investigation of rheological parameters of MRFs under the influence of a magnetic field and at high flow velocities v a special measuring instrument was constructed. New model equations allow the transformation of measured pressure differences Δp and volume flows $\dot{V}$ into the parameters of Bingham viscosity η_B, shear stresses τ, yield points τ_f and shear rates $\dot{\gamma}$. These parameters completely describe the flow of MRFs. For low velocities $v < 1$ cm/s the results agree with data from the MRF producer. For higher velocities v, so far not investigated, the results are plausible. Such high velocities v are relevant for new industrial applications of MRFs, *e.g.*, shock and vibration dampers. The relative permeability μ_r of MRFs shows no frequency dependence for $20 \le f \le 1500$ Hz. Otherwise, μ_r depends on the magnetic field strength H_{ind} and reaches its maximum value $\mu_r \approx 6$ at about $H_{ind} \approx 10^4$ A/m. The described substantial results are obtained in a wide range of parameters and are important for the development and design of modern industrial applicable actuators. The presented miniaturised damper shows the possibilities and limits of the application of MRF.

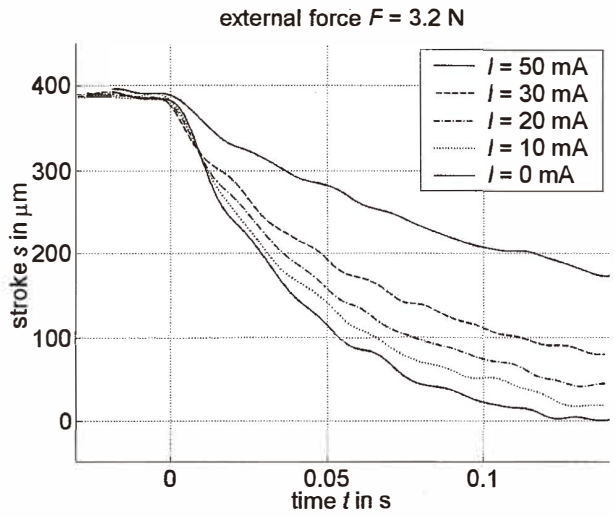

Fig. 16. Measured $s(t)$ curve of the miniaturised end-impact damper.

Acknowledgements

This work was supported by the Saxon Ministry of Economy and Labour (SMWA).

References

1 O. Ashour, C. A. Rogers and W. Kordonsky: Journal of Intelligent Material Systems and Structures **7** (March 1996).
2 W. Kordonsky: J. of Intelligent Materials, Systems and Structures **4** (1993) 65.
3 Y. Grasselli, G. Bossis and E. Lemaire: 6th European Colloid and Interface Society Conf. (1993) p. 175.
4 J. D. Carlson and B. F. Spencer Jr.: Proceedings of the 3rd International Conference on Motion and Vibration Control, Vol. 3 (Japan, Sept. 1996) p. 35.
5 M. R. Jolly, J. D. Carlson and B. C. Munoz: Journal of Smart Materials and Structures **5** (1996) 607.
6 X. Tang and H. Conrad: Quasistatic measurements on a magnetorheological fluid, Journal of Rheology **40** Nov/Dec 1996.
7 L. Richter, U. Lange and L. Zipser: Wiss. Zeitschrift. HTW Dresden **8** (2000) 70.
8 U. Lange, L. Richter and L. Zipser: Wiss. Zeitschrift HTW Dresden **8** (2000) 79.
9 W.-M. Kulicke (Hrsg.): Fließverhalten von Stoffen und Stoffgemischen (Hüthig & Wepf Verlag, Basel, 1986).
10 R. Boll: Weichmagnetische Werkstoffe, Vacuumschmelze GmbH, Verlag Siemens AG, Berlin und München (1990).
11 M. I. Shliomis and V. I. Stepanov: Journal of Magnetism and Magnetic Materials **122** (1993) 176.

12 S. J. Dyke, B. F. Spencer Jr., M. K. Sain and J. D. Carlson: Seismic response reduction using magnetorheological dampers, Proc. IFAC World Congress, June 30–July 5 (1996).
13 X. Wu and M. J. Griffin: Journal of Sound and Vibration **203** (1997) 781.
14 Biedermann Motech GmbH: Beinprothese mit einem künstlichen Kniegelenk mit einer Regeleinrichtung, Offenlegungsschrift Nr.: DE 197 54 690 A 1.